

Scaling flow diagram in the fractional quantum Hall regime of GaAs/AlGaAs heterostructures

S. S. Murzin¹, S. I. Dorozhkin¹, D. K. Maude², and A. G. M. Jansen³

¹ Institute of Solid State Physics RAS, 142432, Chernogolovka, Moscow District, Russia

² Grenoble High Magnetic Field Laboratory, Max-Planck-Institut für Festkörperforschung and Centre National de la Recherche Scientifique, BP 166, F-38042, Grenoble Cedex 9, France

³ Service de Physique Statistique, Magnétisme, et Supraconductivité, Département de Recherche Fondamentale sur la Matière Condensée, CEA-Grenoble, 38054 Grenoble Cedex 9, France

The temperature driven flow lines of the diagonal and Hall magnetoconductance data $(\sigma_{xy}, \sigma_{xx})$ are studied in the fractional quantum Hall regime for a 2D electron gas in GaAs/Al_xGa_{1-x}As heterostructures. The flow lines are rather well described by a recent unified scaling theory developed for both the integer and the fractional quantum Hall effect and predicting universal evolution with temperature of $(\sigma_{xy}, \sigma_{xx})$ for a totally spin-polarized 2D electron system.

PACS numbers:

The scaling treatment was initially proposed for the integer quantum Hall effect (QHE) using a graphical representation of the magnetoconductance data in the form of the flow diagram [1, 2, 3]. The flow diagram depicts the coupled evolution of the diagonal (σ_{xx}) and Hall (σ_{xy}) conductivity components due to interference effects on a distance larger than the diffusion length, when the coherence length increases. The similarity of many features at different integer and fractional quantum Hall states stimulated the creation of unified scaling theories [4, 5, 6, 7, 8]. The results of these theories are in qualitative agreement with each other, however, the phenomenological approach [4, 5, 6, 7] provides a quantitative picture, the experimental verification of which is the goal of our investigation.

In Ref.[4], the conjecture was made that the scaling flow diagram for a totally spin-polarized electron system is invariant under the modular transformation

$$\tilde{\sigma} \leftrightarrow \frac{a\sigma + b}{2c\sigma + d}, \quad (1)$$

for complex conductivity $\sigma = \sigma_{xy} + i\sigma_{xx}$ where a, b, c , and d are integers with $ad - 2bc = 1$. This means that any part of the flow diagram in the $(\sigma_{xy}, \sigma_{xx})$ plane can be obtained from any other part by transformation (1) with corresponding choice of a, b, c , and d . Such transformations can be considered [6] as an extension of the “law of corresponding states” describing the symmetry relations between the different QHE phases [9]. For a holomorphic scaling β -function in the variable $\sigma_{xy} + i\sigma_{xx}$ exact expressions for the shape of the flow lines have been derived [5]. The line shapes are universal, i.e. for a totally spin polarized 2D electron system they do not depend on any parameter of the system such as electron density, disorder, or scattering mechanism.

The structure of the theoretical flow diagram [5], periodic along the σ_{xy} -axis, is shown in Fig .1 for one period $0 < \sigma_{xy} < 1$ (σ_{xx} and σ_{xy} are in units of e^2/h). For $\sigma_{xx} \gg 1$, the points $(\sigma_{xy}, \sigma_{xx})$ flow down vertically with increasing coherence length L , deviate from the vertical at about $\sigma_{xx} \sim 1$, and converge to integer values of σ_{xy}

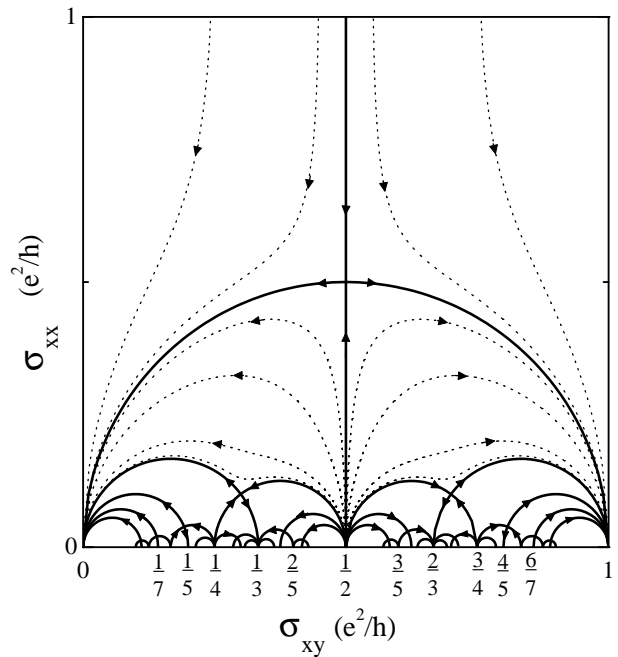


FIG. 1: The scaling flow diagram showing the coupled evolution of the diagonal (σ_{xx}) and Hall (σ_{xy}) conductivity components with increasing coherence length for a totally spin-polarized 2D electron system in the range $0 < \sigma_{xy} < 1$. Solid lines represent the semicircle separatrices and dotted lines give examples of some other flow lines.

(0 or 1 for the range under consideration) on approaching the semicircle separatrix

$$\sigma_{xx}^2 + [\sigma_{xy} - 1/2]^2 = 1/4. \quad (2)$$

The points on the vertical separatrix $\sigma_{xy} = 1/2$, separating different QHE phases, flow vertically to the critical point $(1/2, 1/2)$ both from above and from below. Eq. (1) maps the vertical separatrix at $\sigma_{xy} = 1/2$ into semicircle separatrices connecting pairs of points $(p_i/q_i, 0)$ for integer p_i , and even integer q_i , with flow out from these points. The semicircle separatrix Eq. (2) is mapped

onto semicircle separatrixes connecting pairs of points $(p_i/q_i, 0)$ with odd q_i and flow direction towards these points corresponding to either an integer ($q_i = 1$) or fractional ($q_i > 1$) quantum Hall state, or an insulating state ($p_i = 0$). Crossings of the different type semicircle separatrixes produce the critical points. In these points the conductivity components do not depend on the coherence length. All flow lines different from the separatrixes leave from the points $(p_i/q_i, 0)$ with even q_i and arrive at the points $(p_i/q_i, 0)$ with odd q_i as it shown in Fig. 1 by dotted lines below the large semicircle separatrix of Eq. (2).

An important experimental verification of the scaling theory is possible by measuring the traces on the $(\sigma_{xy}, \sigma_{xx})$ diagram produced by the conductivity components when the temperature is decreased. This idea is based on the temperature dependence of the coherence length, which increases as temperature is decreased. Other changes of the system such as the formation of an energy gap with decreasing temperature are not included in scaling theory. Therefore, to avoid extraneous factors the experiments have to be carried out at rather low temperatures where other system parameters are expected to be temperature independent.

For the integer QHE, the experimentally obtained flow diagram [10] was in qualitative agreement with the theoretical picture. Quantitative agreement between theoretical [5] and experimental flow lines has been found for strongly disordered GaAs layers [11]. To the best of our knowledge the temperature driven flow diagram in the fractional QHE regime has been briefly investigated [12] for $1 < \sigma_{xy} < 2$ only. In this situation, the electron system is not fully spin polarized and the later appeared scaling theory [4] is not directly applicable. However, in a wide variety of samples [13, 14], for the transition from the fractional state $(1/3, 0)$ to the insulating state $(0, 0)$, the value of ρ_{xx} at the temperature independent point has been found to be close to the theoretical critical value $\rho_{xx}^c = h/e^2$.

In the work presented here we explore the temperature driven flow diagram of $\sigma_{xx}(T)$ versus $\sigma_{xy}(T)$ for a 2D electron gas in GaAs/ A_x Ga $_{1-x}$ As heterostructures in the fractional QHE regime with $\sigma_{xy} < 2/3$. A good agreement with the recent scaling theories is found, which implies surprisingly that the evolution with temperature of a totally spin-polarized 2D electron system is universal at low enough temperatures and that the behavior in different parts of the $(\sigma_{xy}, \sigma_{xx})$ plane is connected by simple transformations according to Eq. (1).

Two samples of MBE grown GaAs/ A_x Ga $_{1-x}$ As heterostructures from different wafers were used in our experiments. They have an undoped Al $_x$ Ga $_{1-x}$ As spacer of 50 and 70 nm for sample 1 and 2, respectively. Sample 1, without gate structure, has a low-temperature electron density $n = 1.35 \times 10^{11} \text{ cm}^{-2}$ and a mobility $8.8 \times 10^4 \text{ cm}^2/\text{Vs}$. Sample 2, with a gate structure, has an electron density $n = 1.4 \times 10^{11} \text{ cm}^{-2}$ and a mobility $1.2 \times 10^6 \text{ cm}^2/\text{Vs}$ at zero gate voltage. Previous study of

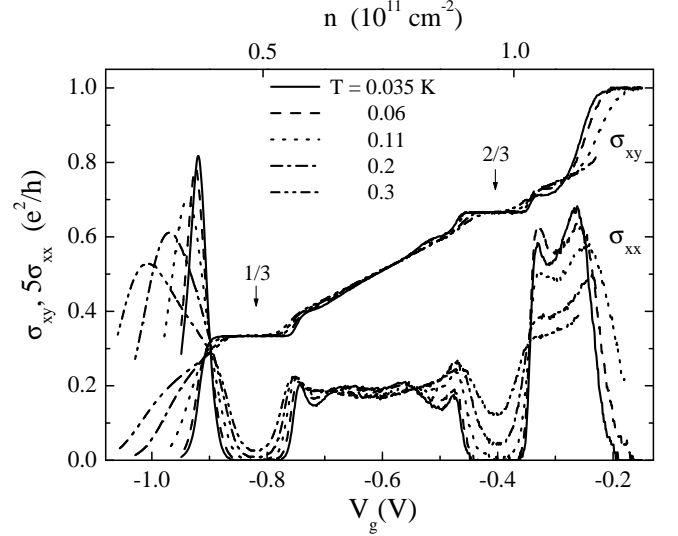


FIG. 2: The diagonal (σ_{xx}) and Hall (σ_{xy}) conductivities as a function of the gate voltage for sample 2 at a 6.0 T magnetic field for different temperatures below 0.3 K. The arrows indicate the gate voltage positions of the σ_{xx} minima for fractional QHE states $2/3$ and $1/3$.

sample 2 [15] proved a spin-depolarization of 2D electron gas at filling factors $2/3 < \nu < 1$, in agreement with theoretical prediction [16]. For this reason we limit the here presented flow diagrams to $0 < \sigma_{xy} < 2/3$. Note that because of very different mobilities of these two samples the same values of σ_{xy} and σ_{xx} at the same temperature are obtained at very different electron densities. For example, the point $(1/2, 0.1)$ for sample 2 is reached at $n \approx 3 \times 10^{10} \text{ cm}^{-2}$, a factor of four smaller than the carrier density in sample 1. The Hall bar geometry was used for measurements of the Hall (ρ_{xy}) and diagonal (ρ_{xx}) resistivities.

For sample 1 without a gate the diagonal (ρ_{xx}) and Hall (ρ_{xy}) resistivities have been measured as a function of the magnetic field B at different temperatures and converted into the $\sigma_{xx}(B)$ and $\sigma_{xy}(B)$ data. The two fractional QHE states ($2/3$ and $1/3$) are well pronounced especially at the lowest temperature. For sample 2 with a gate ρ_{xx} and ρ_{xy} have been measured as a function of the gate voltage V_g at different temperatures for three fixed magnetic fields 2.5, 2.8 and 6 T. The corresponding data for $\sigma_{xx}(V_g)$ and $\sigma_{xy}(V_g)$ (both given in units of e^2/h) are shown in Fig. 2 for $B = 6$ T. The well developed fractional QHE states are observed for $1/3$ - and $2/3$ -filling together with weakly pronounced $2/5$ and $3/5$ states. The upper axis for the electron density n is slightly nonlinear below $n \approx 3 \times 10^{10} \text{ cm}^{-2}$. An additional shallow minimum in σ_{xx} and a step in σ_{xy} can be seen at $n = 1.1 \times 10^{11} \text{ cm}^{-2}$ ($\nu \approx 0.75$). However, their evolution with temperature differs from the usual behavior for the fractional QHE. The value of σ_{xx} in the minimum increases with decreasing temperature and the plateau value of σ_{xy} depends on temperature. This observation is

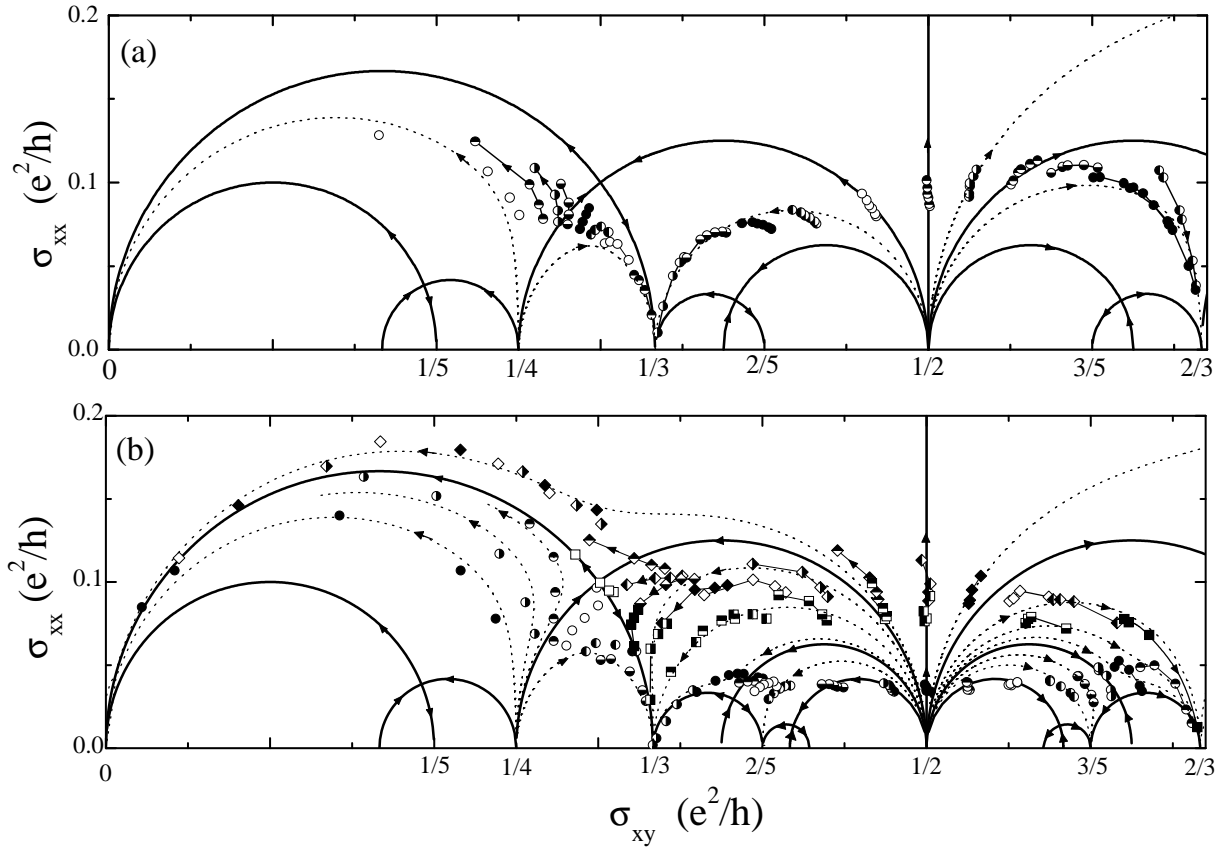


FIG. 3: Flow-diagram of the temperature dependent $(\sigma_{xy}(T), \sigma_{xx}(T))$ data points (a) for sample 1 from 0.37 down to 0.05 K (for $1/3 < \sigma_{xy} < 2/3$) and down to 0.11 K (for $\sigma_{xy} < 1/3$) at different magnetic fields in the range 8.5 – 21 T, and (b) for sample 2 from 0.3 down to 0.035 K at different gate voltages for $B = 2.5$ (diamonds), 2.8 (squares, a few data), and 6 T (circles). Different fillings of the symbols are used for different magnetic fields (data of sample 1) and for different gate voltages (data of sample 2). Solid lines represent the theoretical vertical and semicircle separatrixes. Dotted lines show flow lines close to experimental data.

in agreement with earlier results [17] and probably originates from partial spin polarization of 2DES at filling factors $2/3 < \nu < 1$ which makes the theory [4, 5, 6, 7, 8] inapplicable in this range. At $B = 2.5$ and 2.8 T, the fractional QHE is observed only at $\nu = 1/3$ and $2/3$ as for the data of sample 1.

In Fig. 3, the experimental flow data are compared with theoretical flow diagram and rather good agreement is demonstrated. For sample 1 (Fig. 3(a)) at $\sigma_{xy} = 1/2$ the flow of the experimental data goes vertically up in accordance with the theory. To the left of this line the flow lines deviate to the left and are nearly horizontal around $\sigma_{xy} = 0.4$, before curving down tending to $(1/3, 0)$. Similarly to the right the experimental flow deviates to the right, is almost horizontal around $\sigma_{xy} = 0.6$, and then curves down tending to $(2/3, 0)$. At $0.25 < \sigma_{xy} < 0.3$ the flow lines go approximately up at the beginning and diverge near the critical point close to the theoretically predicted one at $(0.3, 0.1)$.

For sample 2 (Fig. 3(b)), the experimental points reproduce a large part of the theoretical flow lines connecting points $(1/2, 0)$ and $(1/3, 0)$; $(1/2, 0)$ and $(2/3, 0)$;

$(1/4, 0)$ and $(0, 0)$, and follow vertical flow lines at $\sigma_{xy} = 1/2$. The flow line between $(1/2, 0)$ and $(0, 0)$ points also demonstrate very good agreement with the experimental data. Note that the experimental points shift with lowering temperature always in the direction of the nearest flow lines in complete agreement with what is expected from the theory. For example, experimental points move with lowering temperature along the σ_{xx} axis upward in the vicinity of $\sigma_{xy} = 1/2$ and $\sigma_{xy} = 1/4$ and downward in the vicinity of $\sigma_{xy} = 1/3$ and $\sigma_{xy} = 2/3$. The theoretical flow lines directed to fractional QHE states with $\sigma_{xy} = 2/5$ and $\sigma_{xy} = 3/5$ are also rather well confirmed experimentally. A complicated picture exists in the vicinity of the theoretical critical point $(0.3, 0.1)$. Corresponding data are shown in Fig. 4 on an enlarged scale. The experimental data can be well fitted by slightly deforming the separatrix connecting the $(1/2, 0)$ and $(1/4, 0)$ points (dotted line) as is shown by dash-dotted line in Fig. 4. The flow of the experimental data has a nontrivial character: the data points shift towards the critical point when located in the vicinity of the deformed separatrix and away from the critical point along separatrix connecting

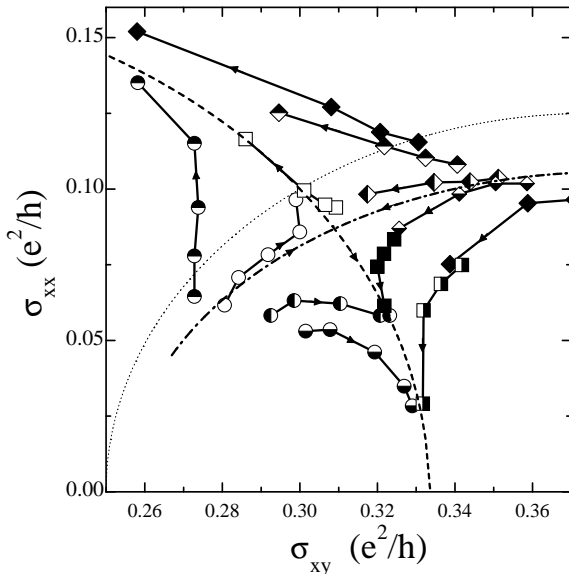


FIG. 4: A part of the flow diagram of Fig. 3(b) in the vicinity of the theoretical critical point $(0.3, 0.1)$. Experimental points (diamonds for $B = 2.5$, squares for 2.8 , and circles 6 T) are connected by solid lines and the direction of their shift with lowering temperature are shown by arrows. The theoretical semicircle separatrices are presented by dashed and dotted lines. Dash-dotted line is obtained by a slight deformation of the dotted theoretical line.

$(1/3, 0)$ and $(0, 0)$ points (dashed line). The separatrix deformation results in shift of the critical point to the $(0.31, 0.09)$ position. Thus, there is only rather small quantitative discrepancy (about 10%) between theoretical and our experimental flow lines. This difference could be attributed to macroscopic inhomogeneity of the sample bearing in mind the data scattering for ρ_{xx}^c , 30% in Ref.[13] and 10% in Ref.[14].

The theoretical flow diagram describes the behavior of a 2D system when only the coherence length depends on temperature with all other parameters being temperature independent. Such regime is obviously limited from both low and high temperature sides. At low temperatures transition to the variable range hopping could break the scaling description. However, this effect would change the flow diagram only in very close vicinity of the quantum Hall states. An estimation of the upper temperature limit for the scaling approach is not well established. Existing experimental results on the temperature dependence of the compressibility of 2DES in the fractional quantum Hall effect regime [18, 19] and non-monotonic temperature dependence of σ_{xx} at $\sigma_{xy} = 1/2$ [20] imply the upper temperature limit for the scaling flow lines to be at approximately 0.5 K. In our samples at temperatures above 0.4 K the deviations of the experimental data from the scaling theory predictions increase gradually, consistently with results of Ref.[18, 19, 20].

In summary, for the fractional quantum Hall effect regime at $0 < \sigma_{xy} < 2/3$ we have found that complicated temperature dependence of the magnetoconductivity tensor components when presented in the form of the flow lines on the $(\sigma_{xy}, \sigma_{xx})$ plane is rather well quantitatively described by equations of the scaling theory [4, 5, 6, 7]. The evolution of $(\sigma_{xy}, \sigma_{xx})$ with decreasing temperature is determined uniquely by the initial values of σ_{xy} and σ_{xx} independently from the microscopic parameters of a totally spin-polarized 2D electron system.

The authors greatly appreciate producing of samples by MBE groups from Institute of Semiconductor Physics RAS, Novosibirsk, Russia (sample 1) and from Max-Planck-Institut für Festkörperforschung, Stuttgart, Germany (sample 2). This work was supported by the *Russian Foundation for Basic Research*.

[1] H. Levine, S. B. Libby, and A. M. M. Pruisken, Phys. Rev. Lett. **51**, 1915 (1983).
[2] D.E.Khmelnitskii, Pis'ma Zh. Eksp. Teor. Fiz. **38**, 454 (1983) [JETP Lett. **38**, 552 (1983)].
[3] A. M. M. Pruisken in *The Quantum Hall Effect*, edited by R. E. Prange and S. M. Girvin, Springer-Verlag, 1990.
[4] C.A. Lütken and G.G. Ross, Phys. Rev. B **45**, 11837 (1992); B **48**, 2500 (1993).
[5] B. P. Dolan, Nucl. Phys. B **554**, 487 (1999); J. Phys. A **32**, L243 (1999).
[6] C.P. Burgess, Rim. Dib, and B.P. Dolan, Phys. Rev. B **62**, 15 359 (2000)..
[7] C. P. Burgess and B. P. Dolan, Phys. Rev. B **63**, 155309 (2001).
[8] A. M. M. Pruisken, M. A. Baranov, and B. Škorić, Phys. Rev. B **60**, 16 807 (1999).
[9] S. Kivelson, D. Lee, and S. Zang, Phys. Rev. B **46**, 2223 (1992).
[10] H. P. Wei, D. C. Tsui, and A. M. M. Pruisken, B 33, 1488 (1986).
[11] S. S. Murzin, M. Weiss, A. G. M. Jansen and K. Eberl, Phys. Rev. B **66**, 233314 (2002).
[12] R. G. Clark, J. R. Mallett, A. Usher, A. M. Suckling, R. J. Nicholas, S. R. Haynes, and Y. Journaux, Surf. Sci. **196**, 219 (1988).
[13] D. Shahar, D. C. Tsui, M. Shayegan, R. N. Bhatt, and J. E. Cunningham, Phys. Rev. Lett. **74**, 4511 (1995).
[14] L. W. Wong, H. W. Jiang, N. Trivedi, and E. Palm, Phys. Rev. B **51**, 18033 (1995).
[15] S. I. Dorozhkin, M. O. Dorokhova, R. J. Haug, and K. Ploog, Phys. Rev. B **55**, 4089 (1997).
[16] T. Chakraborty, Surf. Sci. **229**, 16 (1990).
[17] R. J. Haug, K. v. Klitzing, R. J. Nicholas, J. C. Maan, and G. Weimann, Phys. Rev. B **33**, 4528 (1987)
[18] S. I. Dorozhkin, G. V. Kravchenko, R. I. Haug, K. von Klitzing, and K. Ploog, Pis'ma Zh. Eksp. Teor. Fiz. **58**, 893 (1993) [JETP Lett. **58**, 834 (1994)].
[19] J. P. Eisenstein, L. N. Pfeiffer, and K. W. West, Phys.

Rev. B **50**, 1760 (1994).
[20] L. P. Rokhinson, B. Su, and V. J. Goldman, Phys. Rev. B **52**, 11 588 (1995).